Süleyman Demirel Üniversitesi
Fen Bilimleri Enstitüsü Dergisi
Cilt 29, Sayı 1, 12-20, 2025

Süleyman Demirel University
Journal of Natural and Applied Sciences
Volume 29, Issue 1, 12-20, 2025

DOI: 10.19113/sdufenbed.1560727

The Licochalcone Compound A: Theoretical Studies Applied with DFT Method and Molecular Docking Simulations

Barış KARTAL[1], Aslıhan Aycan TANRIVERDİ*[2], Ümit YILDIKO[3]

[1]Adıyaman Üniversitesi, Gölbaşı Meslek Yüksekokulu, Mülkiyet Koruma ve Güvenlik Bölümü, Adıyaman, Türkiye

[2]Kafkas Üniversitesi, Fen Edebiyat Fakültesi, Kimya Bölümü, 36100, Kars, Türkiye

[3]Kafkas Üniversitesi, Mühendislik ve Mimarlık Fakültesi, Biyomühendislik Bölümü, 36100, Kars, Türkiye

(Alınış / Received: 03.10.2024, Kabul / Accepted: 27.01.2025, Online Yayınlanma / Published Online: 25.04.2025)

Keywords
Licochalcone A,
TD-DFT,
HOMO-LUMO,
Molecular docking

Abstract: Alzheimer's disease (AD) is a health problem that is becoming widespread in the medical sector all over the world. Due to the limited treatment of AD, new clinical candidates are sought. Given the multifactorial nature of AD, an approach targeting the number of regulatory proteins that play a role in the development of the disease is an effective approach. For this reason, interest in different treatment methods has naturally increased in recent years. Medicinal plants and their extracts have been used extensively for the healing of many wounds for years, both professionally and in alternative medicine. Among these natural compounds, these compounds have been of particular interest due to their pharmacological properties such as antioxidants and free radical scavengers. In this study, the molecular geometry, molecular electrostatic potential, and nonlinear optical studies of the Licochalcone A molecule were elucidated by using the density functional theory (DFT) method. In addition, charge transfer within the molecule, HOMO-LUMO energy calculations and Mulliken atomic charge distributions were studied and the results were interpreted with visuals. This analysis also provides drug candidate information about the compound with ligand-receptor binding modes through molecular docking studies.

Licochalcone Bileşiği A: DFT Yöntemi ve Moleküler Yerleştirme Simülasyonları ile Uygulanan Teorik Çalışmalar

Anahtar Kelimeler
Licochalcone A,
TD-DFT,
HOMO-LUMO,
Moleküler yerleştirme

Öz: Alzheimer hastalığı (AD), tıbbi sektörde tüm dünyada yaygınlaşan bir sağlık sorunudur. AD'nin sınırlı tedavisi nedeniyle yeni klinik aday aranıyor. AD'nin çok faktörlü yapısı göz önüne alındığında, hastalığın gelişiminde rol oynayan düzenleyici proteinlerin sayısını hedefleyen bir yaklaşım etkili bir yaklaşımdır. Bu nedenle farklı tedavi yöntemlerine olan ilgi de son yıllarda doğal olarak artmıştır. Şifalı bitkiler ve özleri, hem profesyonel olsun hem de alternatif tıp ile yıllardır bir çok yaraların iyileştirilmesinde çokça kullanılmıştır. Bu doğal bileşikler arasında antioksidanlar ve serbest radikal süpürücüler gibi farmakolojik özellikleri sebebiyle bu birleşiklerle özel olarak ilgilenilmiştir. Bu çalışmada Licochalcone A molekülünün yoğunluk fonksiyonel teorisi (DFT) metodu kullanılarak optimize edilmiş moleküler geometri, moleküler elektrostatik potansiyel ve doğrusal olmayan optik çalışmalar hakkında molekülün yapısı aydınlatılmıştır. Ayrıca molekül içindeki yük transferi, HOMO-LUMO enerji hesaplamaları ve Mulliken atomik yük dağılımları incelendi ve sonuçlar görsellerle yorumlandı. Bu analiz ayrıca moleküler yerleştirme çalışmaları yoluyla ligand-reseptör bağlanma modlarına sahip bileşik hakkında ilaç adayı bilgisi de sağlar.

* Corresponding author: t.aslihanaycan@gmail.com

1. Introduction

There are millions of people living with dementia in today's world, and this number is expected to increase rapidly over the years [1]. Dementia kills a significant number of elderly people[2]. Dementia with Lewy bodies, frontotemporal dementia, and vascular dementia are the three types of dementia that come after Alzheimer's disease (AD), which accounts for 35 million instances of dementia globally [3]. These diseases are considered to be related to AD and can occur as mixed dementia [4]. AD is a developing and neurogenerative disease that causes cognitive impairment, memory loss, and later peripheral problems such as immobility and motor disorders [5]. It has long been thought impossible to find an AD medication that can treat both the pathology and memory loss, despite many attempts. Research employing lecanemab has remarkably demonstrated a cognitive benefit signal, demonstrating the significance of early intervention in pathological circumstances [6]. Some patients who showed abnormalities on brain imaging, such as oedema or haemorrhage, also experienced this impact [6]. The first of several clinical trials targeted at lowering Aβ, these amyloid-based medicines have not been able to appreciably change the course of the disease or clinical symptoms [7]. Treatments aimed at other subpathologies linked to AD, including neuroinflammation, oxidative stress, tau protein-containing neurofibrillary tangles, metabolic and vascular risk factors, and others, have not succeeded [7]. Therefore, there is increasing agreement that the best disease-modifying drug must address multiple aspects of a complex disease.

The degree of cerebral amyloid β peptide (Aβ) accountable [8] for disease is indicated by genetic connections. It is generated through the consecutive proteolytic breakdown of Aβ fragments by two transmembrane proteins, β- and γ secretase [9]. The creation of Aβ and its removal from the cell are not in sync, which causes Aβ to collect into oligomers and plaques. β-secretase and γ-secretase are important targets for the reduction of Aβ [9]. Furthermore, finding molecules that combine good cell penetration with high potency and selectivity has proven to be extremely challenging, even with significant efforts. For this purpose, molecular docking simulations have been tried on compounds used in drug applications extracted from molecules in many studies [10-13].

The use of computer-aided design programs in drug design studies has increased significantly in recent years. The purpose of computer aided drug designs is to assist in the investigation and discovery of the structure of the drug candidate compound [14]. Molecular docking and DFT are two examples of theoretical methods that offer valuable insights into the drug-like characteristics and anticancer behavior of molecular systems [15]. This makes these methods special thanks to the advantages such as not using any chemicals or laboratorymaterials and saving time. DFT allows us to conclude the behavior of the molecule and to characterize molecules because it provides illuminating information about many chemical parameters, such as dipole moment, and chemical potential of HOMO-LUMO orbitals [15]. Molecular docking, on the other hand, allows us to determine how a drug candidate will orient to a different molecule or how they will interact to each other using a molecule's biological activity [15].

In this study, Licochalcone A was obtained from licorice root. Its crucial parameters was determined and elucidated using DFT and Molecular docking methods. Using quantum chemical calculations, the theorical bio characteristics of naturally occurring flavonoids, such Licochalcone A (LCA), were investigated.

2. Material and Method

2.1. Computational study

The theoretical studies were carried out using time-dependent density functional theory (TD-DFT) with B3LYP and B3PW91 functionals, in conjunction with the 6-311G(d,p) basis set. All computations were performed using the Gaussian 09 software package. The analyses included the calculation of HOMO-LUMO energy levels, dipole moments, and Mulliken atomic charges. Geometry optimization was conducted under gas-phase conditions using default convergence criteria, ensuring that the maximum force threshold was below 0.00045 Hartree/Bohr. The visualization of results, including molecular orbitals and charge distributions, was facilitated through the GaussView 6.0 software [16]. Furthermore, molecular docking studies were employed to evaluate the ligand-enzyme interactions and the compound's potential as a protein-binding inhibitor. The Maestro Molecular Modeling platform (Schrödinger, version 11.8) [17] was utilized for these analyses. The LigPrep module was used to generate ligand conformations, while the Protein Preparation Wizard ensured the enzymes were properly preprocessed. The crystal structures of β-Secretase (PDB ID: 3K5F) [18] and γ-Secretase (PDB ID: 7D8X) [19] were obtained from the Protein Data Bank and prepared using the Receptor Grid Generation module. Docking simulations were carried out using Glide's XP docking protocol to determine binding scores and attachment styles. The docking results were further analyzed to identify key interactions within the enzyme active sites, providing insights into the compound's inhibitory potential.

3. Results

3.1. TD-DFT studies

3.1.1. Geometry optimization

The goal of geometry optimization is to know the optimal atomic arrangements that will make the molecule more stable. Adejoro et al. performed calculations on the structure with the lowest energy values. Geometric parameters were obtained after optimization using AM1, PM3, and DFT with the 6-31G and 6-31G* basis sets. Bond distances, bond angles, and dihedral angles were calculated. The PM3 results were found to be better than the AM1 results. It was observed that both methods provided results that were close to the experimental data, but neither could fully explain the stability of the complex. The stability was better described using DFT with the 6-31G and 6-31G* basis sets [20]. Herein, the optimized bond length parameters of the molecule from the DFT calculations [21, 22] using B3LYP/6-311G ++ and B3PW91/6-3011G ++ are shown in Table 1. In the current study, the C-C bond distances for B3LYP were between 1.329 and 1.558 Å; For RB3PW91, these values are between 1,350-1,551 Å. The C-C-H angle in the molecule is between 109° -123°, the H-C-O angles are between 105-106°, the C-C-O angles are between 116° -122° and the C-C-C angles are between 105° and 128°. The values found by the B3LYP and B3PW91 methods are close to each other and are between the expected values.

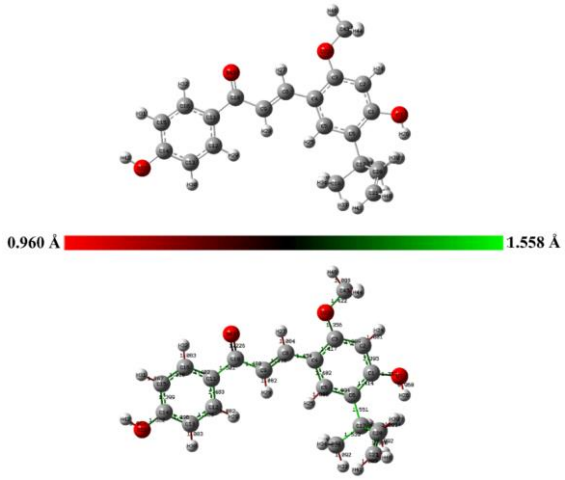

Figure 1. Optimization of Licochalcone A molecule was performed by TD-DFT method using a) B3LYP/6-311G and b) B3PW91/6-311G basis set.

Table 1. The parameters of molecular structure for Licochalcone A by the B3LYP/6-311G ++ (d,p) basis set.

Bond Lengths (Å)			Bond Angles (°)		
Atomic Groups	B3LYP	B3PW91	Atomic Groups	B3LYP	B3PW91
C1-C2	1.396	1.401	C1-C2-C3	120.886	120.204
C1-C6	1.414	1.422	C1-C6-C5	115.551	116.375
C3-O23	1.357	1.384	C1-O7-H26	110.487	112.066
C2-C3	1.390	1.399	C3-C2-H24	122.097	122.408
O23-C43	1.420	1.451	C3-O23-C43	119.143	119.192
C43-H45	1.096	1.098	O23-C43-H46	105.642	105.182
C3-C4	1.417	1.424	H45-C43-H46	111.371	109.769
C5-H25	1.080	1.085	H46-C43-O23	105.642	105.182
C5-C6	1.394	1.401	C17-C19-H38	109.925	109.450
C5-H25	1.080	1.084	H38-C19-H36	108.747	107.973
C4-C8	1.455	1.458	C17-C20-C21	127.486	127.313
C8-H27	1.084	1.088	C20-C21-H41	123.141	122.534
C9-C10	1.480	1.476	H39-C20-C21	116.812	118.681
C10-O47	1.226	1.265	H34-C18-H35	108.625	108.599
C10-C11	1.501	1.499	C8-C4-C5	123.169	123.366
C15-C16	1.386	1.397	C4-C8-C9	128.108	127.480
C13-C14	1.400	1.404	C11-C10-O47	119.530	119.249
C14-O22	1.362	1.391	C10-C11-C12	124.584	124.245
O22-H42	0.963	0.977	C11-C12-H29	120.645	120.811
C14-C15	1.400	1.408	C12-C11-C16	117.918	118.138
C15-H31	1.090	1.089	C11-C16-H32	117.808	117.738
C9-H28	1.082	1.086	C11-C16-C15	121.340	121.341
C1-07	1.368	1.388	C16-C15-H31	120.225	120.170
O7-H26	0.960	0.985	C16-C15-C14	119.851	119.432
C12-H29	1.082	1.086	C15-C14-O22	122.668	122.729
C11-C12	1.403	1.414	C14-O22-H42	109.288	112.329
C12-C13	1.388	1.399	O22-C14-C13	117.570	116.941
C18-H35	1.192	1.097	C14-C13-H30	118.841	118.883
C2-H24	1.081	1.084	C12-C13-H30	121.381	121.555
C17-C19	1.559	1.549	C14-C13-C12	119.778	119.561
C19-H38	1.093	1.096	C13-C12-H29	118.001	117.989
Dihedral Angles (°)			Dihedral Angles (°)		
Atomic Groups	B3LYP	B3PW91	Atomic Groups	B3LYP	B3PW91
C1-C6-C17-C20	61.298	52.710	H28-C9-C8-H27	-178.839	-179.660
C5-C6-C1-O7	179.178	179.923	C8-C9-C10-C11	178.756	-178.276
C1-C2-C3-04	-0.010	0.580	C12-C11-C10-O47	173.352	-174.950
H45-C43-O23-C3	61.265	60.645	C6-C1-O7-H26	6.814	-17.676
H30-C13-C12-H29	0.490	-0.418	H42-O22-C14-C15	0.031	-0.083
H25-C5-C4-C3	-179.994	-179.166	O22-C14-C15-H31	0.003	0.009

The optimized basic structure and total energy conversion of the Licochalcone A [23] molecule are shown in Figure 1.

3.1.2. Molecular electrostatic potential surface (MEPS)

Molecular electrostatic potential surface (MEPS) mapping is used to elucidate the physicochemical properties of the molecule. It is a very illuminating technique to predict the reactive sites of the molecule for nucleophilic and electrophilic attacks on the molecule. Ani et al. calculated the MEP of the compounds in the optimized geometry using B3LYP/6-31G(d,p) to predict the nucleophilic and electrophilic attack sites for Schiff base compounds. From the MEP maps of the compounds, it was determined that the electrophilic and nucleophilic attacks would likely occur at the O1 and N1 sites, as these were the most electronegative and electropositive sites on the maps [24]. The green color refers to the neutral electrostatic potential. The red-colored surfaces define the region of the most negative electrostatic potential, while the blue-colored surfaces represent the region with the strongest attraction force [25]. MEPS maps for the Licochaloce A molecule are shown in Figure 2.

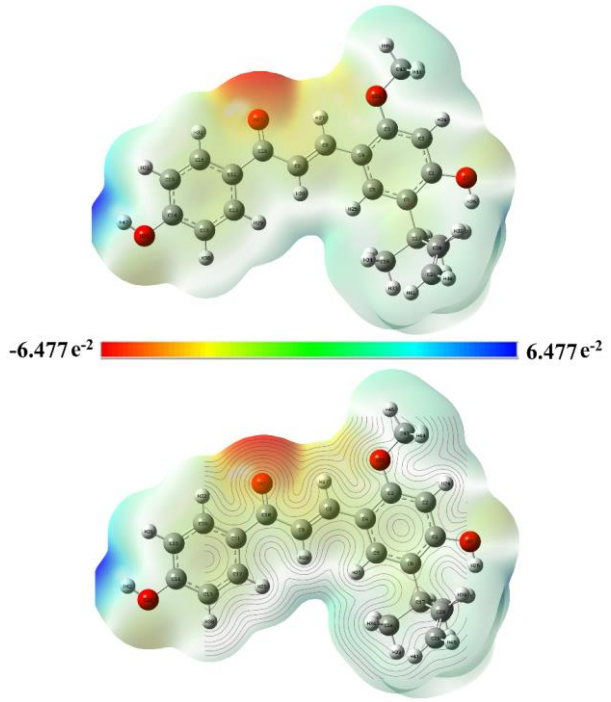

Figure 2. MEPS maps of Licochalcone A molecule were created. They are presented on a scale with color transition values.

3.1.3. Frontier molecular orbitals

The HOMO and LUMO orbitals provide useful information on how the molecule will interact with other species. These orbitals are vital in determining the reactivity and active site portion in reactions based on energy and new electron exchange. LUMO defines electron-accepting capacity while HOMO refers to electron-donating ability [26, 27]. Boundary molecular orbital theory plays an important role in quantum chemistry. The chemical reactivity of a molecule also provides information about its "hardness". If the HOMO-LUMO width value is high, it means that the molecule is hard, while a low value gives important information about whether the molecule is smooth or soft. Molecules with a lower width value are more reactive. HOMO functions as a donor and LUMO as an electron acceptor [28, 29]. Huang et al. listed the calculated frontier orbital energies and the HOMO/LUMO gap for the molecules. They observed an increase in HOMO energy and a decrease in LUMO energy in each system. This resulted in an overall decrease in the HOMO/LUMO gap. This trend was consistent for all five species studied in their research. The reason behind this phenomenon is that exciting electrons to the LUMO level requires more energy, making it more difficult. As a result, the HOMO electrons tend to spread throughout the entire molecule, which facilitates the process [30]. With the DFT method, EHOMO is found to be -5.7090 eV with the B3LYP method, while ELUMO has a value of -1.9108 eV. For the B3PW91 method of Licochalcone A molecule, the EHOMO value was - 5.7901 eV, while the ELUMO value was calculated as - 2.1089 eV. HOMO, LUMO molecular orbital surfaces and energy levels for Licochalcone A molecule are shown in Figure 3 and presented in Table 2. Energy Gap (Δ) |EHOMO- ELUMO| values are calculated as 3.7982 eV and 3.6812 eV, respectively. It can be theoretically stated that it is a semiconductor material [31].

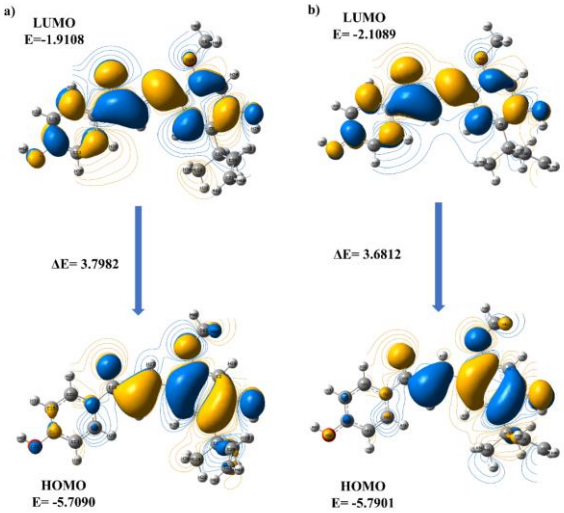

Figure 3. HOMO, LUMO molecular orbital surfaces and energy levels for Licochalcone A molecule B3LYP/6-311G ++ and b)B3PW91/6-311G ++ sets were visualized.

3.1.4. Mulliken atomic charges

The Mulliken atomic charge calculation gives important information about the quantum chemical calculations that play an important role in the application of the molecule to the system. These

calculations provide information about the molecule in light of parameter values such as dipole moment, electronic structure, and molecular polymerization.

Table 2. Electronic parameters for Licochalcone A molecule.

Molecular Energy	B3LYP	B3PW91
E_{LUMO}	-1.9108	-2.1089
E_{HOMO}	-5.7090	-5.7901
E_{LUMO+1}	-0.5534	-0.7396
E_{HOMO-1}	-6.3156	-6.4340
Energy Gap (Δ) $\lvert E_{HOMO} - E_{LUMO} \rvert$	3.7982	3.6812
Ionization Potential ($I = -E_{HOMO}$)	5.7090	5.7901
Electron Affinity ($A = -E_{LUMO}$)	1.9108	2.1089
Chemical Hardness ($\eta = (I - A)/2$)	1.8991	1.8406
Global Softness ($s = 1/2\ \eta$)	0.2632	0.2716
Chemical Potential ($\mu = -(I + A)/2$)	-3.8099	-3.9495
Electronegativity ($\chi = (I + A)/2$)	3.8099	3.9495
Global Electrophilicity ($\omega = \mu^2/2\ \eta$)	3.8216	4.2373

The Mulliken atomic charge distribution indicates the formation of donor and acceptor pairs on the atom, including charge transfer in the molecule [32]. As expected from the available literature results, the Mulliken charges span a very wide range of values at the Hartree-Fock level, from 0.30 on the low side to 0.95 on the high side. Martin et al. observed a similar wide distribution as a function of the basis set in their results for the Mulliken charges calculated using three other quantum mechanical methods [33]. molecular structure of Licochalcone A consists of forty-seven atoms: twenty-one carbon, four oxygen, and twenty-two hydrogen atoms. Mulliken atom was calculated on the basis set B3LYP/6-311G (d,p) and B3PW91/6-311G (d,p) by TDDFT method. These calculations are shown in Table 3 and Figure 4.

3.2. Molecular docking studies

In energy-based active methods, shaped approaches are preferred in the first stage of docking to find solutions [34, 35]. Then, extensive studies can be done on this smaller solution set [36, 37]. The β- and γ-Secretase deep cavity was connected with that of the LCA. The index and body were inserted deep into the cavity, facing the intracellular side (Figure 5). Docking was easier, as there were no conformational changes in an association. This is to be expected given that proteins are modeled as solid bodies and shape is used as the sole criterion for coupling. In all cases, the length is up to a maximum of 7 Å, indicating the role of flexibility in the docking process. Abdullah et al. revealed the interactions between 22 amino acid residues and the Keap1 molecule. The residues ILE421, GLY367, VAL606, ILE559, LEU365, LEU557, ALA510, GLY509, GLY462, GLY364, GLY603, VAL463, VAL418, and GLY419 were involved in van der Waals

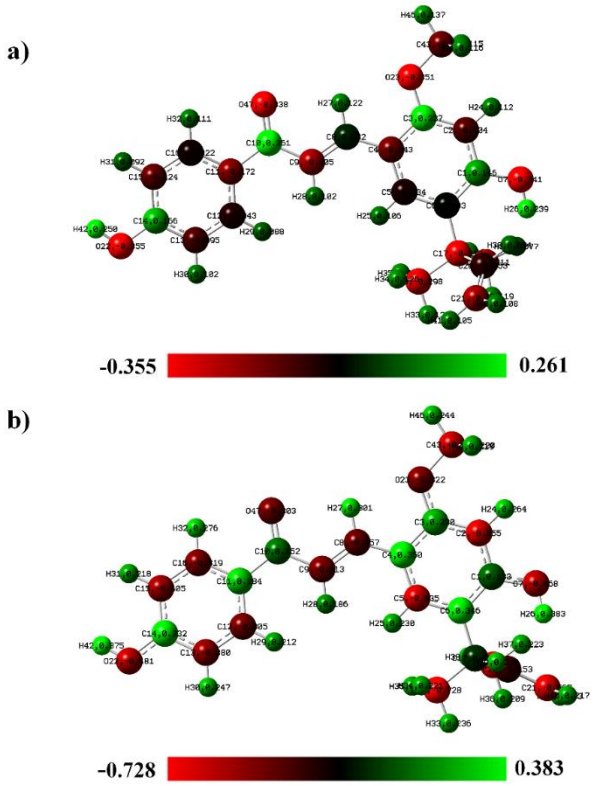

Figure 4. Mulliken atomic charges of licochalcone were tuned at the TD-DFT level using the 6-311G (d,p) basis set of the B3LYP (a) and B3PW91 (b) techniques over a very wide range of values from −0.370 on the low side to 0.30 on the high side.

interactions with the ligand (HST molecule). On the other hand, ARG470, CYS513, CYS368, ALA366, ALA556, and ARG415 formed alkyl and pi-alkyl interactions with the studied molecules and receptors. Additionally, they observed that the amino acids VAL467 and VAL420 participated in pi-sigma interactions with the HST molecule [38].

Certain steps were applied for molecular docking preparation. In the first step, the selected enzymes (β-Secretase (PDB:3K5F) ve γ-Secretase (PDB:7D8X))for protein preparation was downloaded. Then, filled in the missing side chains using prime. The preparation step was optimized, removed waters and minimized respectively. The results of the molecular docking investigation of LCA-β-Secretase show the 2D interaction (Figure 6). Considering the binding mechanism here, LEU-B:30, 4.52 Å (Alkyl, =CH2), TRP-B:115, 5.03 Å (Pi-Alkyl, =CH2) and 5.13 Å (Pi-Alkyl, -CH3), ILE-B:118, 4.77 Å (Alkyl, -CH3), PHE-B:108, 5.49 Å (Pi-Alkyl, =CH2) and 4.64 Å (Pi-Alkyl, -CH3), LYS-B:224, 3.02 Å (Conventional Hydrogen Bond, -OH), THR-B:329, 2.71 Å (Conventional Hydrogen Bond, -H), THR-B:72, 2.45 Å (Carbon Hydrogen Bond, -OH), THR-B:231, 3.09 Å (Carbon Hydrogen Bond, -H) interactions were observed. When the binding mechanism, which is the result of the LCA-γ-Secretase

molecular insertion study, is examined, SER-B:169, 3.07 Å (Carbon Hydrogen Bond, -OH), ALA-B:285, 4.45 Å (Alkyl, -CH3), ILE-B:229, 4.72 Å (Alkyl, -CH3), ILE-B:229, 4.48 Å (Alkyl, -CH3), MET-B:233, 4.07 Å (Alkyl, =CH2), ILE-B:387, 5.44 Å (Alkyl, =CH2), LEU-B: 173, 4.15 Å (Alkyl, -CH3), LEU-B:286, 4.80 Å (Pi-Alkyl,

Table 3. Mulliken atomic charges of Licochalcone.

	B3LYP	B3PW91		B3LYP	B3PW91
C1	0.146	0,132	H25	0.106	0,229
C2	-0.104	-0,554	H26	0.239	0,382
C3	0.237	0,230	H27	0.122	0,301
C4	-0.143	0,350	H28	0.102	0,186
C5	-0.033	-0,534	H29	0.088	0,211
C6	0.003	0,346	H30	0.102	0,246
O7	-0.340	-0,467	H31	0.092	0,218
C8	0.032	-0,256	H32	0.111	0,275
C9	-0.205	-0,313	H33	0.121	0,235
C10	0.261	0,152	H34	0.126	0,221
C11	-0.171	0,283	H35	0.121	0,214
C12	-0.043	-0,305	H36	0.118	0,208
C13	-0.095	-0,379	H37	0.077	0,222
C14	0.166	0,332	H38	0.123	0,229
C15	-0.124	-0,405	H39	0.094	0,249
C16	-0.022	-0,319	H40	0.108	0,217
C17	-0.312	0,061	H41	0.105	0,232
C18	-0.298	-0,727	H42	0.249	0,374
C19	-0.211	-0,713	C43	-0.133	-0,493
C20	-0.053	-0,153	H44	0.115	0,219
C21	-0.198	-0,566	H45	0.115	0,220
O22	-0.355	-0,481	H46	0.137	0,243
O23	-0.351	-0,321	O47	-0.338	-0,303
H24	0.112	0,264	H24		

center of benzene), LEU-B:383, 5.22Å (Alkyl, -CH3) and 2.88 Å (Conventional Hydrogen Bond, =O), GLY-B:384, 1.96 Å (Conventional Hydrogen Bond, =O), LEU-B:268, 5.26 Å (Pi-Alkyl, center of benzene), THR-B:147, 1.97 Å (Conventional Hydrogen Bond, -H) interactions have been reported. On the aromatic surface, the residue-bound areas are close to red, and the body-bound areas are teal. On the H-Bonds surface, the color clustering is different. Donor groups represent purple, acceptor groups represent green [39]. Here, PDB data is entered and some structures are predicted in the algorithm. Some interactions and surface properties are visually presented in Figures 7 and 8. The natural ligand of 3K5F protein is (1R,3S)-3-[1-(acetylamino)-1-methylethyl]-N-[(1S,2S,4R)-1-benzyl-5-(butylamino)-2-hydroxy-4-methyl-5-oxo-pentyl]cyclohexane carboxamide and its binding score was found to be -9.235 kcal/mol. Similarly, the natural ligand of 7D8X protein is 1-[(1S)-1-(4-fluorophenyl)ethyl]-3-[[3-methoxy-4-(4-methylimidazol-1-yl)phenyl]methylidene]piperidin-2-one and its binding score was found to be -9.894 kcal/mol. The docking score in binding affinity of LCA-β-Secretase and LCA-γ-secretase was calculated as

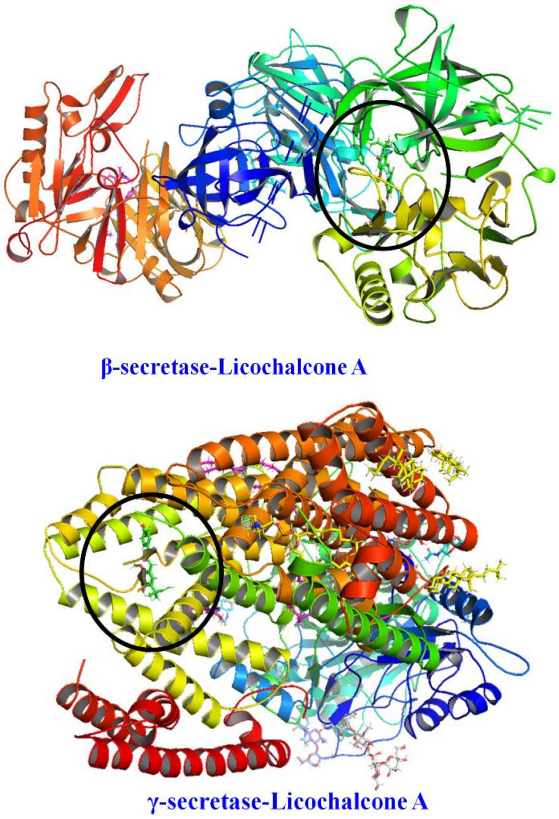

Figure 5. Molecular docking studies were performed. 3D images of LCA-β-Secretase and LCA-γ-Secretase interactions were presented.

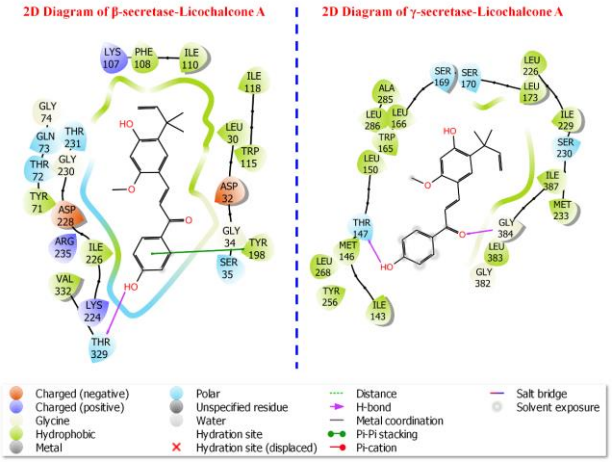

Figure 6. Molecular docking studies were performed. 2D ligand interaction images of LCA-β-Secretase and LCA-γ-Secretase interactions were presented.

-8.536 cal/mol and -8.692 cal/mol, respectively. These values are very close to the binding scores of the natural ligand, underscoring the promising potential of our compound. This similarity in binding affinity suggests that the compound could be an effective candidate for further investigation, as it appears to interact with proteins in a manner comparable to its natural counterpart.

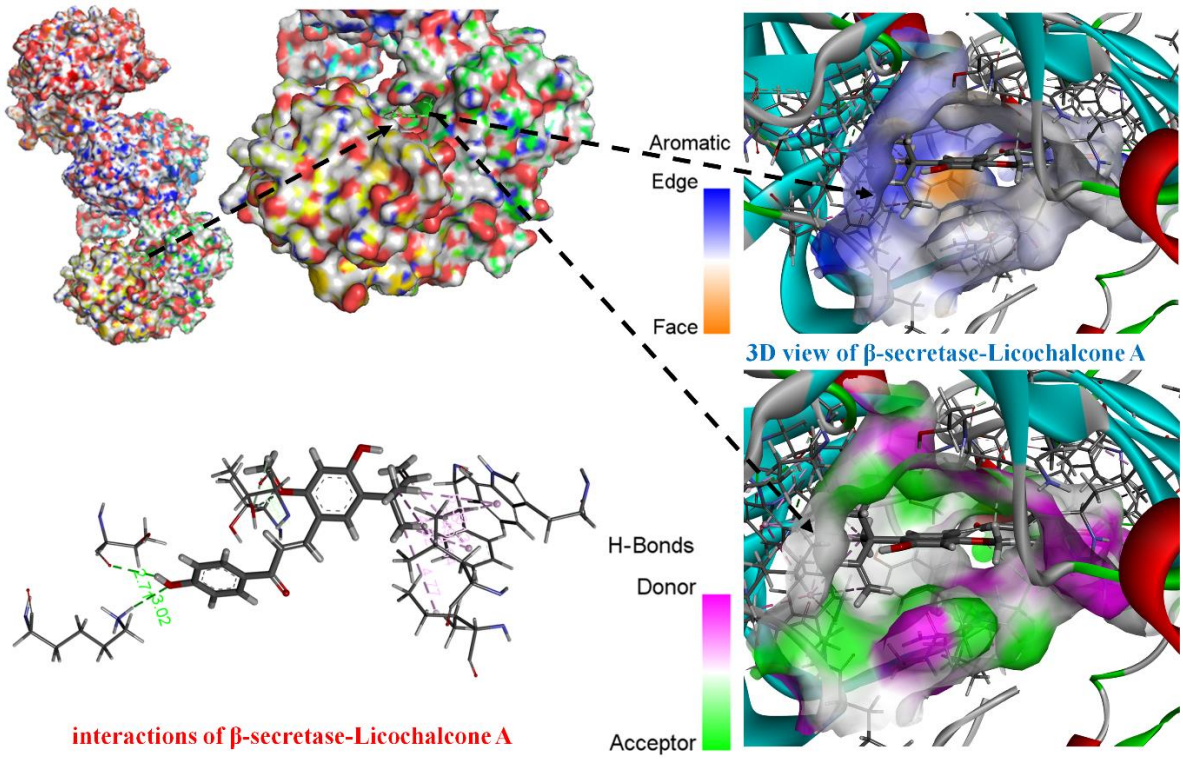

Figure 7. 3D view of the aromatic surface and the hydrogen bonds donor/acceptor surface models of interaction with LCA-β-Secretase enzyme respectively is presented.

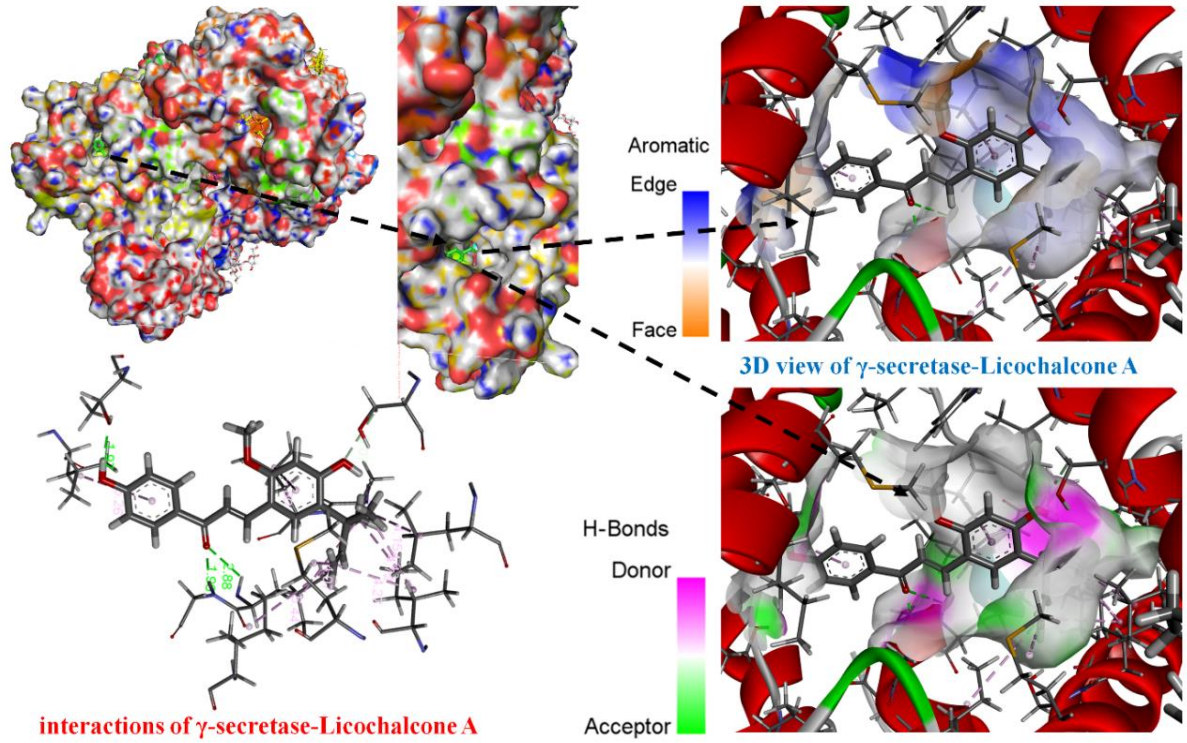

Figure 8. 3D view of the aromatic surface and the hydrogen bonds donor/acceptor surface models of interaction with LCA-γ-secretase enzyme respectively is presented.

3D Views of the aromatic surface (face and edge) and hydrogen bonds (acceptor and donor) surface on the receptor are shown (Figures 7 and 8). Along with the analyses, the receptor molecules investigated by molecular docking technique were detected. LCA-γ-secretase docking analysis was more effective with the receptor-ligand binding score [40].

4. Discussion and Conclusion

This study discusses the molecular structure and biological properties of Licochalcone A, a natural flavonoid, in detail using theoretical methods. The optimized molecular geometry and the calculated HOMO-LUMO energy levels, obtained through TD-DFT, provide crucial data for understanding the chemical reactivity and stability of Licochalcone A. The calculated HOMO-LUMO energy gap of 3.7982 eV with the B3LYP functional suggests that this compound may exhibit semiconductor properties in addition to chemical hardness. The electrostatic potential distribution of the molecule helped identify the nucleophilic and electrophilic interaction sites, thereby presenting the molecule's reactivity map. Molecular docking studies showed that Licochalcone A forms strong and specific interactions with β-Secretase and γ-Secretase enzymes, both of which play significant roles in Alzheimer's disease (AD). A detailed analysis of these interactions revealed several binding mechanisms, including hydrogen bonds, pi-pi interactions, and van der Waals forces. Specifically, the binding energy of -7.228 kcal/mol observed with Gamma-Secretase suggests a promising inhibitory effect on this enzyme. The results indicate that Licochalcone A could be considered as a potential pharmacological agent in the treatment of AD. The theoretical data provided by this study support the role of this natural compound in drug design and development processes. Future in vitro and in vivo studies are essential to confirm these findings and to evaluate the pharmaceutical efficacy of Licochalcone A more thoroughly.

References

[1] Ivosevic, M., et al. 2024 Detection and management of suspected infections in people with dementia – a scoping review of current practices. Ageing Research Reviews, 102520.

[2] Connor, J. 2024. Diagnosis and management of dementia in older people. Medicine, 49(1), 22-25.

[3] Amin, J. and McCausland, B. 2024. Dementia. Medicine, 52(8), 518-521.

[4] Moody, E., et al. 2024. Nursing interventions to improve care of people living with dementia in hospital: A mixed methods systematic review. International Journal of Nursing Studies, 158, 104838.

[5] Carrarini, C., et al. 2024. Neuropsychological and electrophysiological measurements for diagnosis and prediction of dementia: a review on Machine Learning approach. Ageing Research Reviews, 100, 102417.

[6] Marsool, M.D.M., et al. 2023. Newer modalities in the management of Alzheimer's dementia along with the role of aducanumab and lecanemab in the treatment of its refractory cases. Disease-a-Month, 69(5), 101547.

[7] Ding, H., et al. 2022. Cryptotanshinone against vascular dementia through inhibition of Aβ aggregation and inflammatory responses in cerebrovascular endothelial cells. Arabian Journal of Chemistry, 15(12), 104328.

[8] Steiner, H., et al. 2018. Making the final cut: pathogenic amyloid-β peptide generation by γ-secretase. Cell Stress, 2(11), 292.

[9] Schultz, S.A., et al. 2024. γ-Secretase activity, clinical features, and biomarkers of autosomal dominant Alzheimer's disease: cross-sectional and longitudinal analysis of the Dominantly Inherited Alzheimer Network observational study (DIAN-OBS). The Lancet Neurology, 23(9), 913-924.

[10] Torres, P.H., et al. 2019. Key topics in molecular docking for drug design. International journal of molecular sciences, 20(18), 4574.

[11] Ries, M. and Sastre M. 2016. Mechanisms of Aβ clearance and degradation by glial cells. Frontiers in aging neuroscience, 8, 160.

[12] Xu, X. 2009. γ-Secretase catalyzes sequential cleavages of the AβPP transmembrane domain. Journal of Alzheimer's Disease, 16(2), 211-224.

[13] Checler, F., et al. 2021. Is γ-secretase a beneficial inactivating enzyme of the toxic APP C-terminal fragment C99? Journal of Biological Chemistry, 296.

[14] Genç, M., et al. 2022. Synthesis, structural characterization and anticancer activity of 3-(3, 5-dinitrobenzoyl)-1 H-imidazolidine-2-thione. Indian Journal of Chemistry (IJC), 61(2), 201-209.

[15] Genç, M. 2019. Solvatochromic analysis and DFT computational study of N-(hexyl)-N-(5-(3-hydroxynaphthyl-2-yl)-1, 3, 4-oxadiazol-2-yl) amine. Applied Physics A, 125(6), 1-14.

[16] Frisch, M., et al. 2009. Gaussian Inc. Wallingford Ct, 2.

[17] Selvam, C., et al. 2005. Design, synthesis, biological evaluation and molecular docking of curcumin analogues as antioxidant, cyclooxygenase inhibitory and anti-inflammatory agents. Bioorganic & medicinal chemistry letters, 15(7), 1793-1797.

[18] Hanessian, S., et al. 2010. Structure-based design and synthesis of novel P2/P3 modified, non-peptidic beta-secretase (BACE-1) inhibitors. Bioorg Med Chem Lett, 20(6), 1924-7.

[19] Yang, G., et al. 2021. Structural basis of γ-secretase inhibition and modulation by small molecule drugs. Cell, 184(2), 521-533.e14.

[20] Adejoro, I.A. and Oyeneyin, O. 2013. Characterization of a novel polymeric Zinc (II) complex containing the anti-malarial Quinine as ligand: A Theoretical Approach (Semi-empirical

and DFT methods). American Journal of Scientific and Industrial Research, 4, 111-122.

[21] Yİldİko, Ü., et al. 2021. Investigation of novel diethanolamine dithiocarbamate agent for RAFT polymerization: DFT computational study of the oligomer molecules. Bulletin of Materials Science, 44(3), 1-13.

[22] Şen, B., et al. 2016. Synthesis, structural characterization, and DFT calculations of 3-buthyl-4-(3-methyl-3-mesitylcyclobut-1-yl)-1, 3-thiazole-2 (3H)-thione. Crystallography Reports, 61(2), 243-248.

[23] Pandey, P., et al. 2023. A combined experimental and computational chiroptical approach to establish the biosynthesis and absolute configuration of licochalcone L. Phytochemistry, 212, 113732.

[24] Ani, F.E., et al. 2021. Crystal, spectroscopic and quantum mechanics studies of Schiff bases derived from 4-nitrocinnamaldehyde. Scientific Reports, 11(1), 8151.

[25] Karagoz Genç, Z., et al. 2021. The novel tetrahydropyrimidine derivative as inhibitor of SARS CoV-2: synthesis, modeling and molecular docking analysis. Journal of Biomolecular Structure and Dynamics, 10045-10056.

[26] Şenol, Z.M., et al. 2022. Epichlorohydrin and tripolyphosphate-crosslinked chitosan–kaolin composite for Auramine O dye removal from aqueous solutions: Experimental study and DFT calculations. International Journal of Biological Macromolecules, 199, 318-330.

[27] Karabulut, B. and Kirilmiş C. 2020. 5-((4-brom-2-klorfenoksi) metil) oksazolidin-2-on ve 5-((2-brom-4-klorfenoksi) metil) oksazolidin-2-on bileşiklerinin Sentezi ve Teorik Hesaplamaları. Bitlis Eren Üniversitesi Fen Bilimleri Dergisi, 9(2), 500-511.

[28] Karabıyık, H., Kırılmış, C. and Karabıyık H. 2017. Geometry dependence of electron donating or accepting abilities of amine groups in 4, 4′-disulfanediylbis (methylene) dithiazol-2-amine: Pyramidal versus planar. Journal of Molecular Structure, 1141, 650-659.

[29] Yildiko, U. and Tanriverdi, A.A. 2022. A novel sulfonated aromatic polyimide synthesis and characterization: Energy calculations, QTAIM simulation study of the hydrated structure of one unit. Bulletin of the Korean Chemical Society, 43(6), 822-835.

[30] Huang, Y., et al. 2016. Evaluating frontier orbital energy and HOMO/LUMO gap with descriptors from density functional reactivity theory. Journal of Molecular Modeling, 23(1), 3.

[31] Benaissa, M., et al. 2024. Periodic and non-periodic DFT studies of an organic semiconductor material: Structural, electronic, optical, and vibrational properties of ninhydrin. Spectrochimica Acta Part A: Molecular and Biomolecular Spectroscopy, 307, 123636.

[32] Nelson, R., et al. 2020. LOBSTER: Local orbital projections, atomic charges, and chemical-bonding analysis from projector-augmented-wave-based density-functional theory. Journal of Computational Chemistry, 41(21), 1931-1940.

[33] Martin, F. and Zipse, H. 2005. Charge distribution in the water molecule—A comparison of methods. Journal of Computational Chemistry, 26(1), 97-105.

[34] Shree, P., et al. 2022. Targeting COVID-19 (SARS-CoV-2) main protease through active phytochemicals of ayurvedic medicinal plants–Withania somnifera (Ashwagandha), Tinospora cordifolia (Giloy) and Ocimum sanctum (Tulsi)–a molecular docking study. Journal of Biomolecular Structure and Dynamics, 40(1), 190-203.

[35] Yildiko, Ü., et al. 2021. Synthesis, enzymes inhibitory properties and characterization of 2-(bis (4-aminophenyl) methyl) butan-1-ol compound: Quantum simulations, and in-silico molecular docking studies. Journal of the Indian Chemical Society, 98(11), 100206.

[36] Liang, L., et al. 2022. Characterization and molecular docking study of taste peptides from chicken soup by sensory analysis combined with nano-LC-Q-TOF-MS/MS. Food Chemistry, 383, 132455.

[37] TEKEŞ, A.T., et al. 2021. Insilico Molecular Docking Studies of THBF Compound: TD-DFT Simulations and Drug Design. Journal of the Institute of Science and Technology, 11(4), 2955-2966.

[38] Abdullah et al. 2024. Selenium-substituted conjugated small molecule: Synthesis, spectroscopic, computational studies, antioxidant activity, and molecular docking. Journal of Molecular Structure, 1304, 137694.

[39] El-Shalakany, H.H., Ramadan, R.M. and Sayed, M.A. 2024. New bivalent metal chelates based on an NO-donor Schiff base ligand: synthesis, structural characterization, DFT simulation, biological evaluation, and molecular docking analysis. Inorganic Chemistry Communications, 159, 111826.

[40] Swasticharan, L., et al. 2024. A combined metagenome and disease enrichment analysis of nitrosamines present in smokeless tobacco, wiz using molecular docking and functional annotation approach. Gene Reports, 36, 101929.